Photoconductive gain and generation–recombination noise in quantum-well photodetectors biased to strong electric field

V. D. Shadrin and V. V. Mitin
Department of ECE, Wayne State University, Detroit, Michigan 48202

K. K. Choi
U.S. Army Research Laboratory, EPSD, Fort Monmouth, New Jersey 07703-5601

V. A. Kochelap
Institute for Semiconductor Physics, National Academy of Sciences, Kiev 252650, Ukraine

(Received 28 December 1994; accepted for publication 18 July 1995)

The influence of the nonuniform photogeneration on the electric-field distribution is considered for quantum-well photodetectors under drift velocity saturation. We found that spatial nonuniformity of photogenerated electrons due to attenuation of the infrared flux induces strong electric-field domains. The electric-field domains formation is accompanied by degradation of the signal-to-noise ratio. We obtained that domain structures undergo realignment at certain threshold voltage as a result of feedback influence of the quantum well recharging on the photogeneration rates which in turn cause the additional electric-field redistribution. The realignment manifests itself in a steplike change of photoconductive gain and quantum efficiency of photoabsorption at threshold bias voltage and is followed by considerable increase of generation–recombination noise. © *1995 American Institute of Physics.*

I. INTRODUCTION

Recently there has been some progress in understanding the quantum-well infrared photodetectors (QWIPs) performance as far as photoconductive and noise characteristics is concerned. Interesting models have been proposed for photoconductive gain and generation–recombination (GR) noise.[1–4] All these models assumed that electric-field distribution in an active region of a photodetector is uniform. This assumption holds for QWIPs with ideal ohmic contacts and uniform GR rates, but is not valid for nonuniform distribution of generated charge carriers. It has been shown by us in Ref. 5 that photoconductive gain and noise in QWIPs is influenced by attenuation of the infrared flux. The nonuniformity in photogeneration due to flux attenuation induces the charge accumulation in quantum wells in steady-state mode of performance. The quantum-well charging results in a stepwise electric field between wells. In the ohmic region steps of the electric field must repeat the inverse photogeneration function in order to maintain the continuity of the current. In real devices the attenuation of the radiation flux comprises about 1% per period of the quantum-well structure. As a result the steps of the electric field between barriers are small in comparison with the average electric field inside the photodetector.[5] In the multiple-quantum-well structures, however, the small difference of electric field in adjacent domains contributes to remarkable variations of the electric field from cathode to anode.

The QWIPs are best suited to applications in arrays if their collection efficiency and signal-to-noise ratio are as large as possible.[6] The minima of noise is achieved by decreasing it down to value limited by the noise associated with background flux received [background-flux-limited infrared performance (BLIP)]. In BLIP mode of operation the concentration of photogenerated charge carriers prevails over the dark carriers concentration. This emphasizes the importance of the nonuniform photogeneration effects in BLIP. The increase of collection efficiency is realized by increasing the bias voltage at the expense of photoconductive gain increase. The photoconductive gain is proportional to the drift velocity and saturates under strong electric field. In the saturation region small variations in drift velocity needed to compensate changes in concentration of the photogenerated carriers can result in large variations of the electric field in barriers. This can result in strong electric-field domain formation.

In this article we consider an electric field of arbitrary intensity assuming the saturation of drift velocity, i.e., we exploit the commonly accepted model of the vertical transport in the quantum-well structures. We investigate the domain formation under infrared radiation attenuation and consider the influence of electric-field domains on photoconductive gain and noise characteristics. We also consider the GR noise as a main source of noise in QWIPs.[6] In contrast to the domain formation in superlattices due to resonant tunneling between different subbands of adjacent wells,[7] we examine the domain formation in the absence of tunneling. For this purpose we consider wide barriers separating wells and assume drift transport of charge carriers in barriers over the quantum wells while generation and recombination occur in the narrow well regions separating barriers. We consider n-type doped quantum wells with one two-dimensional subband of confined electron states. The photogeneration occurs from the ground subband of confined electrons to the extended states over the barriers. This type of quantum-well detector is widely used in applications.[6]

II. PHOTOCONDUCTIVE GAIN

We consider N quantum wells (QWs) equally separated by barriers with spatial period l. The equations for current density and electron concentration has been derived in Ref. 5

 0021-8979/95/78(9)/5765/10/$6.00

for the model of QWIP we consider here. We neglect the width of the QWs in comparison with the barriers' width and actually replace the equation for electrons in the vicinity of the QW by the boundary condition imposed on the electron concentration in the plane of the QW location. It was shown in Ref. 5 that diffusion component of the electron current can be neglected in electric field of interest. The equations in the drift approximation are given by

$$\frac{1}{e}\,\mathrm{div}\,\mathbf{j}=\sum_{i=1}^{N}\{g_i-[n(x)-n_0]s_i\}\delta(x-x_i), \tag{1}$$

$$j_x=env_d(x), \tag{2}$$

where j_x is the xth component of the electron current density vector $\mathbf{j}=(j_x,0,0)$, $n(x)$ is the volume density of electrons in extended states, n_0 is the equilibrium density, s_i is the rate of capture of electrons into confined states, $\delta(x)$ is the delta function, and $v_d(x)$ is the drift velocity of electrons. The value of s_i is analogous to the recombination velocity on interfaces containing QWs. It can be expressed via lifetime τ_i of nonequilibrium electrons in extended states over the ith barrier: $s_i=l/\tau_i$. It is known both theoretically and experimentally[8,9] that carrier capture time into QWs exhibits oscillation as a function of QW width being typically of the order of several picoseconds of it minimal value in GaAs–AlGaAs QW structures.

Here we assume the drift velocity dependency upon electric field $E(x)$ to be equal to

$$v_d=\frac{\mu E(x)}{\sqrt{1+[\mu E(x)/v_s]^2}}, \tag{3}$$

where $E(x)$ is the electric field, μ is the electron mobility, and v_s is the saturation velocity.

In order to find a steady-state electric-field distribution in the lack of illumination we have to solve the Poisson equation for electric field $E(x)$ with boundary conditions imposed on electric field. We assume instead that contacts are ohmic and represent both contacts as QWs of an unlimited capacity of electrons with a cathode contact covering any deficit in electron concentration without deterioration of its injection capability. In this case the electric field is uniform and QWs retain neutrality. All the charge is placed in the contacts, the cathode being charged by negative and anode by positive charge which can be calculated by using the formula for a capacitor,

$$Q_{ss}=V_B\epsilon/(4\pi L),$$

where V_B is the bias voltage and L is the distance between contacts ($L=lN$ in the case considered). In what follows we consider effects associated with quantum wells located inside the structure between contacts under illumination.

The continuity of the current density in different barriers should be taken into consideration in steady state. After integration of Eq. (1) over the slab which includes the ith quantum well we obtain by using current continuity $j_{i+1}=j_i$

$$n_i-n_0=g_i/s_i, \tag{4}$$

where j_i is the xth component of current density in ith barrier which separates the $(i+1)$th and ith QWs.

It was shown in Ref. 5 that charge accumulated in QWs under nonuniform photogeneration is rather small in the ohmic region and does not significantly influence photogeneration rates. Considering a strong electric field we have to take into account the dependency of the generation rates upon concentration of the excess electrons accumulated in wells.

For this purpose we consider the linear concentration dependency of the photogeneration rates g_i. The relation between generation rates g_i with accumulated sheet density $\Delta N_i=N_i-N_i^{(0)}$ and uniform generation rates $g_i^{(0)}$ corresponding to $N_i=N_i^{(0)}$ is given by

$$g_i-g_i^{(0)}=g_i^{(0)}(\Delta N_i/N_i^{(0)}). \tag{5}$$

The excess accumulated charge $\Delta Q_i=e\Delta N_i$ is related to the electric fields E_i in the barriers. This follows from the Poisson equation integrated over the QW region,

$$E_i-E_{i-1}=\frac{4\pi e}{\epsilon}\Delta N_i. \tag{6}$$

In this manner we use Poisson equation by substituting the expression for excess accumulated electron charge ΔN_i from Eq. (6) into Eq. (5) for generation rates g_i. It is worth remembering here that in our model the Debye length for electrons exceeds the sample length as happens in real QWIPs and the electric-field distribution is determined by the charge accumulation in the contacts and in the QWs. We find the sheet concentration of electrons in the QW by

$$N_i^{(0)}=N_{ss}E_F=\frac{m^*}{\pi\hbar^2}\,\theta_iE_{\mathrm{photo}}, \tag{7}$$

where N_{ss} is the density of states in the ground subband of the QW, m^* is the effective mass of electrons in the subband, and θ_i is the ith QW filling factor, which is equal to the ratio of the Fermi energy E_F to the energy E_{photo} of the photoionization threshold. By substituting the expression for N_i^0 into the equation for photogeneration rates we obtain the equation for g_i:

$$g_i=g_i^{(0)}[1+(E_i-E_{i-1})/E_c(i)], \tag{8}$$

where the electric field E_c characteristic for accumulated charge is determined by

$$E_c(i)=\frac{4\theta_iE_{\mathrm{photo}}}{ea_B^*}. \tag{9}$$

Here a_B^* is the effective Bohr radius for electrons,

$$a_B^*=\frac{\epsilon\hbar^2}{m^*e^2}.$$

The characteristic electric field E_c depends upon initial filling factor θ_i of the ith QW. The typical electron concentrations in wells correspond to $\theta\simeq0.1$–0.3. For a detector based on GaAs–AlGaAs with the long-wavelength cutoff $\lambda_c=10$ μm ($E_{\mathrm{photo}}=0.124$ eV) we obtain the typical value of the characteristic electric field,

$$E_c\simeq5\times10^4\ \mathrm{V/cm}.$$

Next we consider high photogeneration rates, $g_i \gg n_0 s_i$, i.e., the BLIP mode of operation. The formula for current density in ith barrier follows from Eqs. (2)–(4),

$$\left(\frac{1}{e}\right) j_i = \frac{g_i v_i}{s_i}, \tag{10}$$

where v_i is the drift velocity in the ith barrier. The rate of photogeneration g_i equals

$$g_i = \Phi_i \eta_0,$$

where Φ_i is the photon flux at $x = x_i$, and η_0 is the quantum efficiency of photoabsorption of the single QW, i.e., the probability of one photon to be absorbed by one QW while passing through it.

The photoconductive gain, according to definition, equals

$$G = \frac{j_i}{e\Phi_0 \eta} = \frac{j_i}{e\Sigma_{i=1}^{N} g_i} = \frac{v_i g_i}{s_i \Sigma_{i=1}^{N} g_i}. \tag{11}$$

Making equal current densities in two barrier regions adjacent to the ith QW, we obtain the relation between drift velocities in ith and $(i+1)$th barrier layers,

$$v_i g_i / s_i = v_{i+1} g_{i+1} / s_{i+1}. \tag{12}$$

In the presence of the nonuniform absorption ($g_i \neq g_{i+1}$) or fluctuations of recombination velocities ($s_i \neq s_{i+1}$) the drift velocities in ith and $(i+1)$th barriers should be different in order to satisfy continuity of current. This is realized by setting different electric fields in barriers induced by QW recharging.[5] We have to emphasize that here as in Ref. 5 we consider a photodetector with ideal ohmic contacts incorporating the uniform distribution of the electric field in the absence of illumination.

The average electric field $\langle E \rangle$ in the detector active region equals

$$\langle E \rangle = \frac{1}{N} \sum_{i=1}^{N} E_i. \tag{13}$$

From Eq. (3) we obtain the relation between electric field and drift velocity in the ith barrier,

$$E_i = \frac{v_i}{\mu \sqrt{1 - (v_i / v_s)^2}}. \tag{14}$$

Using Eq. (10) we express the electric field in the ith barrier via current density,

$$E_i = \frac{g E_s}{\sqrt{(g_i^* / s_i^*)^2 - g^2}}, \tag{15}$$

where $g = G\langle s \rangle N / v_s$, $E_s = v_s / \mu$, $g_i^* = g_i / \langle g \rangle$, $s_i^* = s_i / \langle s \rangle$. Here the angled brackets mean averaging over the well sites,

$$\langle k \rangle = \frac{1}{N} \sum_{i=1}^{N} k_i.$$

Substituting Eq. (15) into Eq. (13) we obtain the equation for the determination of g,

$$\frac{1}{N} \sum_{i=1}^{N} \frac{g}{\sqrt{(g_i^* / s_i^*)^2 - g^2}} = \frac{\langle E \rangle}{E_s}. \tag{16}$$

For the uniform generation $g_i = \langle g \rangle = \eta / N (g_i^* = 1)$ and for the ideal QWs $s_i = \langle s \rangle (s_i^* = 1)$ the electric field in barriers is uniform $E_i = \langle E \rangle$. In this case we obtain from Eq. (16) the simple equation for the photoconductive gain,

$$\frac{g}{\sqrt{1 - g^2}} = \frac{\langle E \rangle}{E_s}.$$

For uniform electric field the photoconductive gain equals

$$G = v_d(\langle E \rangle) / N \langle s \rangle, \tag{17}$$

where

$$v_d(\langle E \rangle) = \frac{\langle E \rangle}{\mu \sqrt{1 + (\langle E \rangle / E_s)^2}}.$$

In the case of a weak electric field, i.e., $g_i^* / s_i^* \gg g$, we find

$$g = \frac{\langle E \rangle}{E_s (1/N) \Sigma_{i=1}^{N} s_i / g_i},$$

which can be converted to

$$G = \frac{\langle v \rangle}{N \langle s \rangle} \frac{1}{(1/N) \Sigma_{i=1}^{N} g_i (1/N) \Sigma_{i=1}^{N} s_i^* / g_i}. \tag{18}$$

This equation almost coincides with the equation for photoconductive gain obtained in Ref. 5 for the ohmic region of current–voltage dependency. The distinction between Eq. (18) and the corresponding formula in Ref. 5 lies in geometric fluctuations of the recombination velocities included in Eq. (18). It is worth considering uniform generation in Eq. (18), i.e., $g_i = \langle g \rangle$, then taking into account $\langle s^* \rangle = 1$ we obtain

$$G = \frac{\langle v \rangle}{N \langle s \rangle}.$$

The previous equation can be obtained from Eq. (17) under the condition $\langle E \rangle \ll E_s$.

Next we consider the solution of Eq. (16) under the condition $\langle E \rangle \gg E_s$, i.e., for very strong electric field assuming that the generation rates are not influenced significantly by the electrons accumulated in the wells. We restrict our consideration to structures illuminated from the cathode side.

In order to satisfy Eq. (16) with $\langle E \rangle \gg E_s$ the value of g should be close to the minimum value of g_i^* / s_i^*. Let us assume for definiteness sake that there are no fluctuations of the recombination velocity from well to well, i.e., $s_i^* = 1$. In the case of illumination from the cathode side structure the generation rates g_i^* take a minimum value by $i = N$. The approximate solution of Eq. (16) in this case may be obtained by equaling the last term in the sum to right-hand side of Eq. (16),

$$\frac{1}{N} \frac{g}{\sqrt{(g_N^*)^2 - g^2}} \simeq \frac{\langle E \rangle}{E_s}. \tag{19}$$

After simple algebra we obtain

$$G \simeq \frac{G_s N g_N}{\eta \sqrt{1+(E_s^2/N^2\langle E\rangle^2)}} \simeq \frac{G_s N g_N}{\eta}. \tag{20}$$

For a detector without a back-reflecting mirror (one pass of the radiation flux) we obtain $g_i=\Phi_0(1-\eta_0)^{i-1}\eta_0$, where photon flux Φ_0 entering the first ($i=1$) QW can be expressed through external flux Φ_s. For the radiation input which employs a prism we have a correspondence $\Phi_0=(1/2)\Phi_s \sin^2\theta$. Quantum efficiency for one pass equals

$$\eta=\frac{\Sigma_{i=1}^{N} g_i}{\Phi_s}=\frac{1}{2}[1-(1-\eta_0)^N]\sin^2\theta. \tag{21}$$

For a detector with a back-reflecting mirror (double pass of the radiation flux) we obtain

$$g_i=\Phi_0\eta_0[(1-\eta_0)^{i-1}+(1-\eta_0)^{2N-i-1}].$$

Quantum efficiency for double pass equals

$$\eta=\tfrac{1}{2}[1-(1-\eta_0)^{2N}]\sin^2\theta. \tag{22}$$

The proof of correctness of solution (20) for photoconductive gain is given in the Appendix.

We obtain an analytical formula for photoconductive gain for two radiation input geometries by using Eq. (20).

A. One pass of infrared radiation

For one-pass geometry of the radiation input we obtain, using Eqs. (20) and (21),

$$G=\frac{v_s}{\langle s\rangle N}\frac{N\eta_0(1-\eta_0)^{N-1}}{1-(1-\eta_0)^N}. \tag{23}$$

This equation is valid for an arbitrary number of wells N. For a multiple QW structure, by using relation

$$(1-\eta_0)^N \simeq \exp(-\eta_0 N),$$

which is correct for $\eta_0 \ll 1$ and $N \gg 1$, we obtain

$$G=\frac{v_s}{\langle s\rangle N}\frac{N\eta_0\exp(-\eta_0 N)}{1-\exp(-\eta_0 N}. \tag{24}$$

In the case of weak absorption $\eta_0 N \ll 1$ we obtain from Eq. (30)

$$G=G_s=\frac{v_s}{\langle s\rangle N}.$$

This formula is different from those obtained for the uniform generation. This distinction is due to different distributions of the electric field corresponding to uniform absorption and the latter formula obtained for a strong electric-field domain occupying the Nth barrier adjacent to the anode.

B. Double-pass of infrared radiation

We obtain from Eqs. (20) and (21) for double pass

$$G=G_s\frac{2N\eta_0(1-\eta_0)^{N-1}}{1-(1-\eta_0)^{2N}}. \tag{25}$$

For a multiple QW photodetector we obtain

$$G=G_s\frac{2N\eta_0\exp(-\eta_0 N)}{1-\exp(-2\eta_0 N)}. \tag{26}$$

It is worth noting that in the case of weak absorption the photoconductive gain for double pass is the same as for one-pass radiation input geometry. This can be explained by the identical electric-field distribution we considered in both cases, i.e., the bias voltage drops entirely across the last barrier adjacent to anode contact.

We considered solutions for the electric fields in barriers neglecting the influence of accumulated charge in wells on the photogeneration rates. Now we estimate the conditions imposed on bias voltage and device parameters under which this influence can be neglected for the strong electric-field domain occupying Nth barrier. It is evident from Eq. (8) that accumulated charge does not significantly influence the photogeneration rate in Nth well if the inequality

$$E_N-E_{N-1}<E_c(N)$$

is satisfied. For strong electric-field domain occupying Nth barrier this enequality reads

$$\frac{V_B}{l}<E_c(N), \tag{27}$$

where V_B is the bias voltage, which drops almost entirely on the Nth barrier. By using Eq. (9) the latter inequality can be presented as

$$\frac{eV}{E_{\text{photo}}}\frac{a_B^*}{4l}<\theta. \tag{28}$$

In the case of typical filling factor $\theta \simeq 0.1$–0.3, corresponding to the doping impurity concentration $N_D=(10^{17}$–$10^{18})$ cm^{-3}, this inequality can be satisfied for $V_B<1$ V provided that width of the barrier is of the order of $l=10^{-5}$ cm. This value of the bias voltage may be not large enough to achieve a high value of the ratio $\langle E\rangle/E_s$.

The situation is different in the ohmic region ($\langle E\rangle \ll E_s$). In this case the electron sheet concentration accumulated in the ith quantum well produces an electric-field step, which equals[5]

$$E_i-E_{i-1}=\frac{g_{i-1}^{(0)}-g_i^{(0)}}{g_i^{(0)}}E_{i-1}\simeq E_i\eta_0.$$

Taking into account that in the ohmic region the electric-field domains are weak, i.e., $E_i \simeq \langle E\rangle = V/lN$, we obtain that the condition $E_i-E_{i-1}<E_c(i)$ will be satisfied under less stringent requirements imposed on device parameters than those for strong electric field. We obtain

$$\frac{eV_B}{E_{\text{photo}}}\frac{a_B^*}{4l}\frac{\eta_0}{N}<\theta. \tag{29}$$

This inequality can be easily satisfied in low-biased structures.

Before considering the domain formation self-consistently by taking into account the influence of accumulated charge on electric-field distribution it is worth describing the procedure of noise current calculation.

III. NOISE CURRENT AND NOISE GAIN FACTOR

The main source of noise in QW infrared detectors is the GR noise. The GR noise and relevant noise gain has been

considered in Refs. 2–4 for uniform electric-field distribution and in Ref. 5 for weak electric-field domains in the ohmic region of the current–voltage characteristics.

In this article we consider the Langevin-type equation for fluctuations in the drift approximation in the electric field of arbitrary strength. The equation for low-frequency fluctuations averaged over the coordinates of the points in the plane perpendicular to the superlattice axis is formulated as[5]

$$\left(\frac{1}{e}\right)\frac{d\delta j_x}{dx}=\sum_{i=1}^{N}\left[-\delta n(x)s_i+\delta g_i-\delta r_i\right]\delta(x-x_i), \quad (30)$$

where the x component of the averaged in-plane current density fluctuation equals

$$\delta j_x(x)=\delta j_i=ev_i\delta n_i+e\mu n_i\delta v_i(x), \quad x_i\leqslant x\leqslant x_{i+1}. \quad (31)$$

Here δg_i and δr_i are the Langevin sources for fluctuation of generation and recombination rates, $\delta v_i(x)$ is the fluctuation of electron drift velocity in the ith barrier, and $\delta n_i=\delta n(x_i)$. Equations (30) and (31) are analogous to the corresponding equations for GR fluctuation derived by us for QW structure in the ohmic region of the current–voltage characteristic. We use these equations here to consider drift velocity saturation in the strong electric field.

For stationary fluctuations we have an equality

$$\delta n_i=(\delta g_i-\delta r_i)s_i^{-1}.$$

After integration of Eq. (30) over the $x_{i-1}<x<x_{i+1}$ we obtain

$$\delta j_i-\delta j_{i-1}=-s_i\delta n_i+\delta g_i-\delta r_i=0, \quad i=1,2,\ldots,N. \quad (32)$$

Estimation shows that the electric field produced by the concentration of free electrons in the barriers can be neglected and $\delta E(x)=\delta E_i$ for $x_i\leqslant x\leqslant x_{i+1}$. From Eq. (31) we obtain

$$\delta v_i=\frac{\mu\delta E_i}{[1+(\mu E_i/v_s)^2]^{(3/2)}}=\frac{\delta j-ev_i\delta n_i}{en_i}, \quad (33)$$

where $\delta E_i(x)$ is the fluctuation of electric field $E_i(x)$ in the ith barrier, and $\delta j=\delta j_i$. We used in Eq. (33) the formula

$$\frac{dv_i}{dE_i}=v_i'=\left[1-\left(\frac{\mu E_i}{v_s}\right)^2\right]^{(3/2)}.$$

For stabilized bias voltage across a sample we obtain

$$\sum_{i=1}^{N}\delta E_i=0.$$

After substitution of δE_i from Eq. (33) into the previous equation we obtain the expression for current density fluctuation,

$$\delta j=\frac{e\Sigma_{i=1}^{N}(v_i/v_i')(\delta n_i/n_i)}{\Sigma_{i=1}^{N}(v_i'n_i)^{-1}}. \quad (34)$$

The general approach to evaluation of correlation functions of noise sources δg_i and δr_i is developed in Ref. 10 for spatially homogeneous systems. For processes concentrated in very narrow well regions we follow Ref. 11 and express the correlation functions via recombination velocity s_i and concentration of free electrons n_i over wells,

$$\langle\delta g_i\delta g_k\rangle_\omega=\langle\delta r_i\delta r_k\rangle_\omega=2n_is_iA^{-1}\delta_{ik},$$

$$\langle\delta g_i\delta r_k\rangle_\omega=0,$$

where A is the detector cross-section square and $n_i=g_is_i^{-1}+n_0$,

$$\delta\langle j^2\rangle_\omega=e^2\frac{\Sigma_{i=1}^{N}(v_i/v_i')^2n_i^{-2}(4n_is_i^{-1}A^{-1})}{[\Sigma_{i=1}^{N}(v_i')^{-1}n_i^{-1}]^2}. \quad (35)$$

The mean square current noise in the frequency bandwidth Δf equals

$$\langle\delta I^2\rangle=\langle\delta j^2\rangle_\omega A^2\Delta f. \quad (36)$$

For homogeneous thermal generation $n_i=n_0$ and $s_i=\langle s\rangle$ the electric field is uniform, i.e., $E_i=\langle E\rangle$, $v_i=v_d(\langle E\rangle)$, and we obtain from Eqs. (35) and (36)

$$\langle\delta I^2\rangle=4eG_0I_T\Delta f,$$

where $I_T=ev_d(\langle E\rangle)n_0A$ is the dark thermal current.

Next we consider background-limited infrared performance, when photogeneration rates exceed thermogeneration rates, i.e., $g_i\gg n_0s_i$. After substituting $n_i=g_is_i^{-1}$ into Eq. (35) we obtain

$$\langle\delta I^2\rangle_\omega=\frac{4I_p^2}{A}\frac{\Sigma_{i=1}^{N}[1+(E_i/E_s)^2]^3g_i^{-3}s_i^2}{\{\Sigma_{i=1}^{N}[1+(E_i/E_s)^2]^{3/2}g_i^{-1}s_i\}^2}, \quad (37)$$

where we use Eq. (10) for current density in order to obtain photocurrent I_p,

$$ev_ig_iA/s_i=I_p.$$

Following Ref. 1 we introduce the coefficient F between photoconductive gain G and noise gain G_n; the latter is determined by

$$\langle\delta I^2\rangle_\omega=4eG_nI_p. \quad (38)$$

Using the definition of the photoconductive gain

$$G=\frac{I_p}{e\Phi_s\eta A}=\frac{I_p}{eA\Sigma_{i=1}^{N}g_i}$$

we obtain the equation for excess noise gain factor $F=G_n/G$,

$$F=\frac{\Sigma_{i=1}^{N}[1+(E_i/E_s)^2]^3g_i^{-3}s_i^2\Sigma_{i=1}^{N}g_i}{\{\Sigma_{i=1}^{N}[1+(E_i/E_s)^2]^{3/2}g_i^{-1}s_i\}^2}. \quad (39)$$

Using Eq. (15) we obtain

$$\sqrt{1+(E_i/E_s)^2}=\frac{g_i\langle s\rangle}{N\eta s_ig}\frac{E_i}{E_s}. \quad (40)$$

We find from Eqs. (39) and (40)

$$F=\frac{\Sigma_{i=1}^{N}g_i^3s_i^{-4}E_i^6\Sigma_{i=1}^{N}g_i}{[\Sigma_{i=1}^{N}(g_i^2s_i^{-2}E_i^3)]^2}. \quad (41)$$

For the ohmic region we obtain from Eq. (12)

$$E_ig_i/s_i=\text{const}. \quad (42)$$

Substituting $E_i=\text{const}\times(s_i/g_i)$ we find, instead of Eq. (41),

$$F=\frac{\Sigma_{i=1}^{N}g_i^{-3}s_i^2\Sigma_{i=1}^{N}g_i}{[\Sigma_{i=1}^{N}(g_i^{-1}s_i)]^2}. \quad (43)$$

For $s_i=\langle s\rangle$ this formula coincides with the formula for excess noise gain factor derived in Ref. 5, otherwise this equation permits us to calculate the factor F for structure with geometric noise caused by fluctuations of the recombination velocity. In the case of uniform illumination we obtain from Eq. (43), by using Eq. (42),

$$F=\frac{N\Sigma_{i=1}^{N}s_i^2}{(\Sigma_{i=1}^{N}s_i)^2}=\frac{\langle s^2\rangle}{(\langle s\rangle)^2}. \tag{44}$$

It follows from Eq. (44) that $F\leqslant 1$. Thus, the geometrical fluctuations of recombination velocity lead to the decrease of GR noise. In reality, changes of capture velocity caused by variations in well width or well depth are accompanied by changes of the photoabsorption probability. This makes it difficult to separate the influence of the recombination rates fluctuation from the nonuniform absorption effects.

Next we obtain an analytical formula for the excess noise coefficient in the framework of the validity of the analytical solution (20) for photoconductive gain; then $\langle E\rangle/E_s\gg 1$ and bias voltage drops on the last barrier, so that $E_N\simeq V/l$, and $E_i\ll E_N$ for $i\neq N$. Because electric field in other barriers is smaller in comparison with E_N, the negative charge, which normally should be placed on a cathode, will be concentrated in the Nth QW. Other QWs are charged with sufficiently smaller charge which is distributed among them according to Eq. (6).

A. One pass of infrared radiation

Using equations for η and g_N in one-pass geometry of radiation input we obtain

$$F=\frac{1-(1-\eta_0)^N}{\eta_0(1-\eta_0)(N-1)}. \tag{45}$$

For a multiple QW structure this equation can be presented as

$$F=\frac{\exp\ \eta_0 N-1}{\eta_0}. \tag{46}$$

For $N\eta_0\ll 1$ but $N\eta_0>(E_s/\langle E\rangle)^2$ we find

$$F\simeq N. \tag{47}$$

B. Double pass of infrared radiation

The formula for the excess noise coefficient F in this case is

$$F=\frac{1-(1-\eta_0)^{2N}}{2\eta_0(1-\eta_0)^{(N-1)}}. \tag{48}$$

For a multiple QW structure we obtain

$$F=\frac{sh(\eta_0 N)}{\eta_0}. \tag{49}$$

For $N\eta_0\ll 1$ and $N\eta_0>(E_s/\langle E\rangle)^2$ it follows from Eq. (A1) in the Appendix that

$$F\simeq N. \tag{50}$$

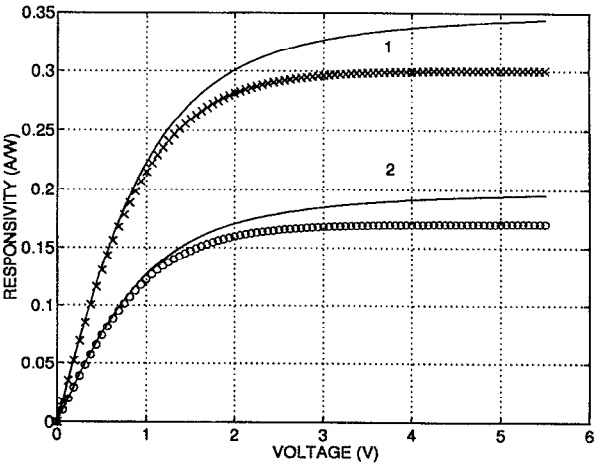

FIG. 1. Voltage dependency of the (1) responsivity and (2) photoconductive gain for nonself-consistent approach. Solid line: uniform generation; x and circles: nonuniform generation, $\eta=0.218$.

IV. SELF-CONSISTENT CONSIDERATION OF PHOTOCURRENT AND NOISE

As we indicated earlier the solutions obtained by neglecting the influence of charge accumulated in wells on the photogeneration are of limited usage. Here we consider the influence of the accumulated charge on the photogeneration rates and find the electric-field distribution by solving Eqs. (8) and (16) for electric field and gain simultaneously. In addition to calculation of quantum efficiency η and photoconductive gain G we calculate responsivity R which is determined by

$$R_\lambda=\frac{e\lambda}{hc}G\eta, \tag{51}$$

where λ is the wavelength of radiation received, h is the Planck constant, and c is the light velocity. The detectivity of the photodetector in the BLIP is proportional to the ratio

$$D^*\propto\sqrt{\eta/F},$$

and is not dependent upon photoconductive gain.[12] In what follows we calculate the dimensionless value of $S_N=\sqrt{\eta/F}$ which is proportional to the signal-to-noise ratio.

We choose characteristic saturation field $E_s=5\times10^3$ V/cm and electron mobility $\mu=2\times10^3$ cm^2/V s. We use the value of capture time $\tau=5$ ps. The calculations are made for a structure which consists of $N=50$ heavy-doped QWs with electron filling factor $\theta=0.4$. This corresponds to a single QW efficiency of photoabsorption $\eta_0=0.02$.[13] In this case the parameter $N\eta_0$ is equal to $N\eta_0=1$. The distance between QWs is assumed to be $L=500$ Å. The quantity of the characteristic electric field E_c corresponding to the chosen parameters equals $E_c=2\times10^5$ V/cm. We performed all calculations for GaAs–AlGaAs QW photodetector with the long-wavelength cutoff $\lambda=10$ μm.

The results of the responsivity and photoconductive gain calculations are shown in Fig. 1. These calculations are made in the framework of a nonself-consistent approach. The solid line curve corresponds to the case of uniform photogenera-

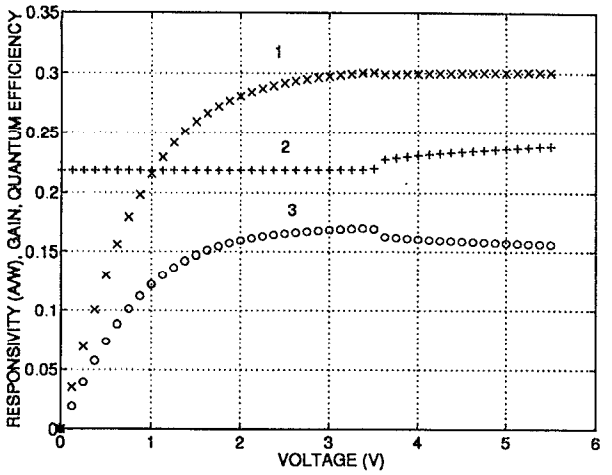

FIG. 2. Voltage dependency of (1) responsivity, (2) quantum efficiency, and (3) photoconductive gain calculated by using the self-consistent approach.

tion with $\eta_0=\eta/N$ and $g_i=\Phi_0\eta_0$. The difference in results corresponding to uniform and nonuniform absorption is attributed entirely to the difference in photoconductive gain G. For bias voltage $V_B=5$ V the photoconductive gain for attenuated infrared flux is about 15% smaller in comparison with gain calculated for the uniform photogeneration. Quantum efficiency for double pass equals $\eta=22\%$ and is not dependent upon voltage in both cases.

Figure 2 displays results of R_λ, G, and η calculations based on self-consistent consideration. Noteworthy are steps in quantum efficiency and photoconductive gain at $V_B\simeq 3.4$ V. They are due to realignment of the electric-field domains in the vicinity of the anode.

This realignment results in changes of the electric-field distribution, which induce the steplike increase of quantum efficiency due to additional absorption by electrons accumulated in the QWs adjacent to the anode and steplike decrease of photoconductive gain. The steplike decrease of photoconductive gain stems from sensitivity of the gain to the changes of the photogeneration function in the vicinity of the anode. Contrary to steplike changes of η and G the value of responsivity, which is proportional to the product ηG, remains unchanged.

The electric-field distributions in barriers are shown in Fig. 3 for different bias voltages. The distributions corresponding to the self-consistent solution are shown in Figs. 3(a)–3(c). We choose three bias voltages which are equal to

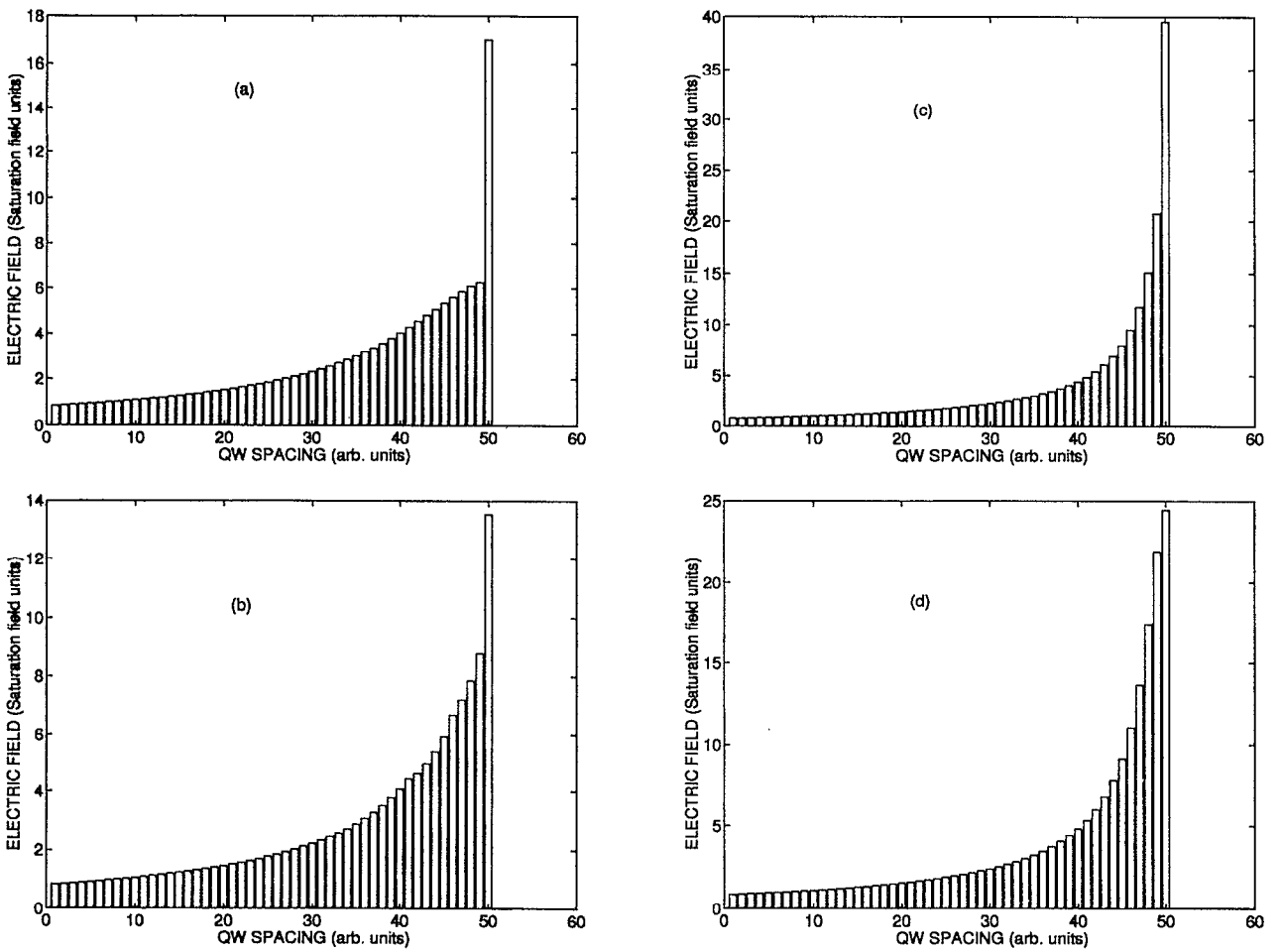

FIG. 3. Electric-field distribution for different bias voltages: (a) at threshold $V_B=3.375$ V, $\eta=0.221$, $G=0.160$; (b) above threshold $V_B=3.600$ V, $\eta=0.223$, $G=0.158$; (c) above threshold $V_B=5.00$ V, $\eta=0.238$, $G=0.153$; (d) nonself-consistent approach $V_B=5.00$ V, $\eta=0.218$, $G=0.170$.

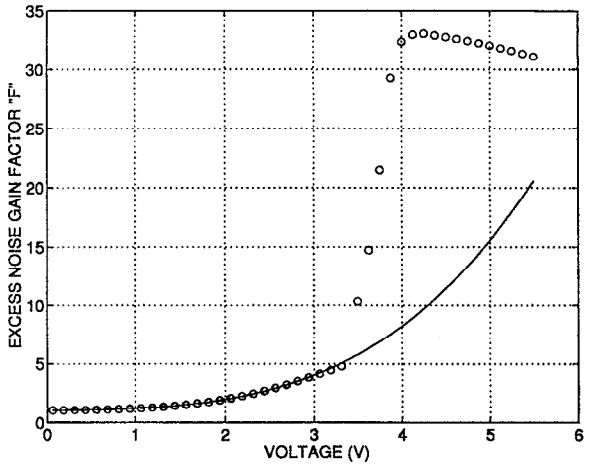

FIG. 4. Excess noise gain factor as the function of bias voltage. Solid line: nonself-consistent approach; circles: self-consistent calculations.

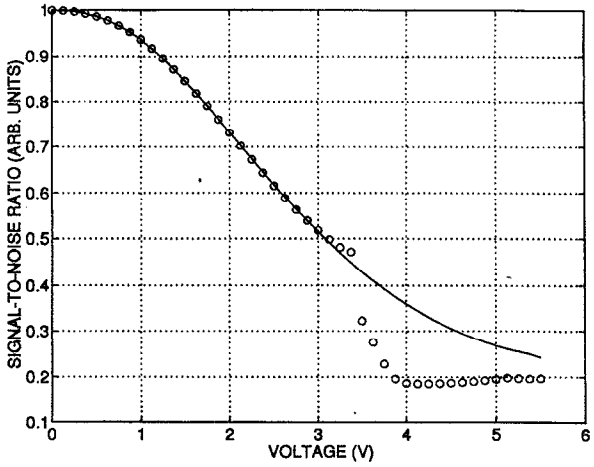

FIG. 5. Voltage dependency of the signal-to-noise ratio. Solid line: nonself-consistent approach; circles: self-consistent calculations.

(a) the threshold value of bias corresponding to the beginning of realignment $V_B=3.4$ V [Fig. 3(a)],
(b) the value slightly higher than threshold $V_B=3.6$ V [Fig. 3(b)], and
(c) the value far enough from threshold $V_B=5.0$ V [Fig. 3(c)].

The distribution corresponding to the nonself-consistent solution is shown for comparison for bias voltage $V_B=5$ V in Fig. 3(d). The electric field in the Nth barrier undergoes the abrupt change at the threshold voltage due to negative charge accumulation in the Nth QW adjacent to the anode. With the voltage increase above threshold the electric-field distribution shown in Fig. 3(a) transforms into a set of the strong electric-field domains with comparable strength located near the anode. The distribution shown in Fig. 3(b) is typical for domains at bias voltages above threshold. The evolution of the electric-field domains with the voltage increase [Fig. 3(b)] produces electric-field distribution with more contrast domains near the anode as compared to the nonself-consistent solution [Fig. 3(d)].

The realignment of electric-field domains results in a significant variation of the noise characteristics. The excess gain factor F is depicted in Fig. 4 for $E_c \to \infty$ (solid line) and $E_c=2\times10^5$ V/cm (circles). First, it is noteworthy to mention the significant increase of F for the nonself-consistent solution (solid line) under bias voltage corresponding to the drift velocity saturation. Second, the electric-field domain realignment [Figs. 3(a),3(b)] results in sharp increase of the excess noise gain factor F at the threshold. The sharp increase of the F factor gives way to its stabilization within several tenths of volts after the threshold voltage. For the bias voltage over $V_B=4$ V both self-consistent and nonself-consistent F factors tend to draw close together. Under bias voltage $V_B>5.5$ V the electric field in the Nth domain for self-consistent solution is so large that tunneling from the ground subband of the Nth quantum well can be significant. To be in the framework of the exploited model we calculated all quantities for bias voltage which do not exceed $V_B=5.5$ V. The signal-to-noise ratio which is shown in Fig. 5 has been calculated for two above-discussed cases. The decrease in S_N at threshold bias is followed by two curves approaching closer together.

Only several strong-field domains determine noise in the region $V_B>4$ V where stabilization occurs for the self-consistent solution. The difference between self-consistent and nonself-consistent solution for electric field tends to diminish as bias voltage recedes far enough from the threshold. Simultaneously, this leads to the gap decrease between two F factors corresponding to a self-consistent and nonself-consistent solution.

V. CONCLUSIONS

We applied the existing concept of QWIP and processes of electron transport in it to calculations of the photoconductive and noise characteristics. Two major features of the model widely accepted in the current description of QWIPs[6] has been accounted for in calculations performed in this article. We took into account that

(a) contacts are ohmic, and
(b) drift velocity saturates under strong electric field.

The first feature assumes the uniform electric-field distribution inside the structure with lack of illumination, and the second results in the strong electric-field domain formation under bias voltage corresponding to the saturation region of the current–voltage characteristic. For the purpose of clarity it should be mentioned that ohmic contacts do not guarantee uniformity of the electric-field distribution inside a structure. The deviation from the charge neutrality in QW structures and electric-field domain formation in the dark can be provoked by the bulk mechanisms of the charge transport such as the sequential resonant tunneling between two electron subbands in the adjacent QWs.[7,14–16] We assume in our model that the width of the barriers is large enough to prevent the electron tunneling processes. We also consider temperatures low enough to maintain BLIP mode of operation even in the strong electric fields. In this case the transport of

electrons in the illuminated structure is determined by the photogenerated charge carriers moving in the three-dimensional conduction states over the barriers. We do not address in this article the influence of the thermogeneration, thermotunneling, or tunneling of electrons on the electric-field domains formation in QWIPs. Although important, these varieties of the electron transport can be separated from the transport of photogenerated electrons by lowering the operating temperature of the photodetector. Less obvious is the assumption about the ideality of the contacts. The deviation from the ideal ohmic behavior can result in excess charge accumulation (depletion) near the contacts in the dark. The model of ideal ohmic contacts is widely accepted in the existing descriptions of QWIPs.[6] The theory we present here is aimed at better understanding of QWIPs characteristics in the framework of this model.

We also find that formation of domains significantly influences noise gain. Basically, the noise gain is larger in value than that of the photoconductive gain. The distinction between both gains drastically increases if the strong electric-field domains occur under influence of attenuation of the infrared radiation in the drift velocity saturation region. The experimental results based on independent determination of both gains do not show significant difference in both gains.[1,17] The experimental results do not contradict our theory in ohmic region where excess noise gain happens to be larger than photoconductive gain as has been observed in Ref. 17. However experimental evidence of the photocurrent saturation exists which could result in the framework of our model with the occurrence of strong electric-field domains and in an increase of GR noise. It is unclear, however, if the assumption of ideal ohmic contacts is satisfied in real QWIPs. If contacts display blocking behavior, the uniform electric-field distribution cannot be realized even under uniform generation. In this case the depletion of quantum wells in the region adjacent to the cathode is possible in order to eject electrons and maintain the continuity of current. This depletion can result in the saturation of photocurrent at the expense of the quantum efficiency decrease. Thus, our results call for a revision of the physical model of QWIP in case the photocurrent saturation is not followed by the noise increase.

In the framework of the exploited model the performance of the QWIP displays a large variation of excess noise gain factor F and signal-to-noise ratio as a function of bias voltage in the drift velocity saturation region. The attenuation of the infrared radiation flux induces the electric-field domains and charge accumulation in the QW which in turn influences the photogeneration rates. The electric-field dependency of the photogeneration rates is more pronounced in the vicinity of the anode where attenuation takes it maximum. The feedback between photogeneration and electric-field distribution results in a realignment of the electric-field domains near the anode at some threshold bias voltage. The realignment begins with significant (of the order of 20% of its initial value corresponding to the initial filling of the QW) charge accumulation in the Nth QW adjacent to the anode [Fig. 3(a)]. With the further voltage increase the strong electric-field domain which occupies the last barrier decays into several domains of comparable strength located near the anode [Fig. 3(b)]. Contrary to the photoconductive *gain* which is not influenced considerably by this process, the noise characteristics which are sensitive to the electric-field distribution display large variations in process of domain realignment. Before threshold all the characteristics calculated self-consistently coincide well with those calculated beyond the self-consistent scheme. The noise gain factor increases drastically at the threshold bias voltage corresponding to the onset of the domain structure realignment. The noise characteristics above the threshold tend to draw together to nonself-consistent solution.

On the other hand the noise characteristic calculated in framework of the nonself-consistent approach with attenuation of the radiation flux taken into account is very different from characteristics specific for uniform photogeneration. We estimated a full range variation of the excess noise gain factor F from $F=1$ up to $F=N$, depending upon bias voltage applied to the structure. Thus, we get the conclusion that QWIPs' noise characteristics under high bias voltage may be very sensitive to the nonuniformity of illumination, depending upon the sublinearity of the electric-field dependency of the drift velocity. From this point of view the quantum-well structures that feature the largest values of characteristic saturation electric field E_s offer advantages for reduced noise performance under high bias voltage as compared to structures with smaller E_s even if the low-field mobility of the latter structures is superior to those with larger characteristic electric field E_s.

APPENDIX

In order to check a validity of solution (20) we estimate the ratio of sum of the remaining terms of Eq. (16) (i.e., $E_{i<N}/E_s$) to the last term (i.e., E_N/E_s).

For one-pass geometry of radiation input we obtain

$$g_i^2=g_N^2/(1-\eta_0)^{2(N-i)}. \tag{A1}$$

Substituting this into formula (15) for electric field in ith barrier we obtain

$$E_i/E_s=\frac{(1-\eta_0)^{(N-i)}}{N\sqrt{1-(1-\eta_0)^{2(N-i)}}}. \tag{A2}$$

Replacing the sum

$$\sum_{i=1}^{i=N-1}\frac{E_i}{E_s}$$

with the integral

$$\int_{x=1}^{x=N} dx\,\frac{E_x}{E_s},$$

we estimate the sum and compare it to the ratio E_N/E_s.

It is convenient to present the function E_x as

$$E_x=\frac{\exp[-x\,\ln(1-\eta_0)]E_s}{N\sqrt{\exp[-2N\,\ln(1-\eta_0)]-\exp[-2x\,\ln(1-\eta_0)]}}. \tag{A3}$$

Taking into account that $\eta_0 \ll 1$ we use approximations

$$\ln(1-\eta_0)\simeq-\eta_0.$$

After substitution,

$$y=\exp(x\eta_0),$$

we obtain

$$I=\frac{1}{E_s}\int_1^N dx\ E_x \rightarrow \frac{1}{\eta_0 N}\int_1^{\exp(N\eta_0)} dy\ \frac{1}{\sqrt{1-y^2}}. \tag{A4}$$

Finally, we obtain

$$\sum_{i=1}^{N-1}\frac{E_i}{E_s}=I=\frac{1}{\eta_0 N}[\arcsin[\exp(-N\eta_0)] - \arcsin[\exp(-2N\eta_0)]. \tag{A5}$$

For $N\eta_0 \gg 1$ we obtain

$$\frac{\Sigma_{i=1}^{N-1}E_i}{E_N}\simeq\frac{E_s}{\langle E\rangle}\frac{\exp(-N\eta_0)}{N\eta_0}\ll 1. \tag{A6}$$

The last inequality can be valid even for $\langle E\rangle/E_s \cong 1$.

For $N\eta_0 \ll 1$ we obtain

$$\frac{\Sigma_{i=1}^{N-1}E_i}{E_N}\simeq\frac{E_s}{\langle E\rangle}\left(\frac{1}{N\eta_0}\right)^{1/2}. \tag{A7}$$

To obtain Eq. (A7) we used the approximation ($x \ll 1$)

$$\arcsin(1-x)\simeq(\pi/2)-\sqrt{2x}.$$

Finally, we conclude that the approximation we used to solve Eq. (16) is valid for one pass of infrared radiation for $N\eta_0 \ll 1$ if condition $N\eta_0 \gg (E_s/\langle E\rangle)^2$ is satisfied. For $N\eta_0 \gg 1$ the solution (20) is valid for a wide range of the fields ratio $\langle E\rangle/E_s$, including $\langle E\rangle/E_s \simeq 1$.

Analogous estimations made for double-pass geometry of the radiation input produce the same conditions imposed on the device parameters in order to satisfy solution (20) of Eq. (16).

[1] B. F. Levine, A. Zussman, S. D. Gunapala, M. T. Asom, J. M. Kuo, and W. S. Hobson, J. Appl. Phys. **72**, 4429 (1992).
[2] W. A. Beck, Appl. Phys. Lett. **63**, 3589 (1993).
[3] H. C. Lui, Appl. Phys. Lett. **61**, 2703 (1993).
[4] K. K. Choi, Appl. Phys. Lett. **65**, 1266 (1994).
[5] V. D. Shadrin, V. V. Mitin, V. A. Kochelap, and K. K. Choi, J. Appl. Phys. **77**, 1771 (1994).
[6] B. F. Levine, J. Appl. Phys. **74**, R1 (1993).
[7] K. K. Choi, B. F. Levine, R. J. Malik, J. Walker, and C. G. Bethea, Phys. Rev. B **35**, 4172 (1987).
[8] J. A. Brum and G. Bastard, Phys. Rev. B **33**, 1420 (1986).
[9] A. Fujiwara, S. Fukatsu, Y. Shiraki, and R. Ito, Surf. Sci. **263**, 642 (1992).
[10] K. M. van Vliet and J. R. Fassett, in *Fluctuation Phenomena in Solids*, edited by R. E. Burges (Academic, New York, 1965), Chap. 7.
[11] V. A. Kochelap, V. N. Sokolov, and N. A. Zakhleniuk, Phys. Rev. B **48**, 2304 (1993).
[12] A. Rose, in *Concepts in Photoconductivity and Allied Problems* (Wiley-Interscience, New York, 1963).
[13] F. L. Serzhenko and V. D. Shadrin, Sov. Techn. Lett. **15**, 171 (1991).
[14] A. Shakouri, I. Grave, Y. Xu, A. Ghaffari, and A. Yariv, Appl. Phys. Lett. **63**, 1101 (1993).
[15] S. H. Kwok, R. Merlin, H. T. Grahn, and K. Ploog, Phys. Rev. B **50**, 2007 (1994).
[16] J. Kastrup, H. T. Grahn, K. Ploog, F. Prengel, A. Wacker, and E. Scholl, Appl. Phys. Lett. **65**, 1808 (1994).
[17] B. Xing, H. C. Lui, P. H. Wilson, M. Buchanan, Z. R. Wasilewski, and J. G. Simmons, J. Appl. Phys. **76**, 1889 (1994).